crystals

MDPI

Article

Synthesis, Crystal Structures, and Properties of Two Coordination Polymers Built from Imidazolyl and Carboxylate Ligands

Xing-Zhe Guo, Zhi-You Zhang, Zi-Long Li, Shan-Shan Shi and Shui-Sheng Chen *

College of Chemistry & Chemical Engineering, Fuyang Normal University, Fuyang 236041, China; zhujjj1993@126.com (X.-Z.G.); zhaodiliu@126.com (Z.-Y.Z.); njncwater@163.com (Z.-L.L.); fuyangnu@163.com (S.-S.S.)

* Correspondence: fyuniv@163.com; Tel.: +86-558-259-5836

Academic Editor: Shujun Zhang

Received: 6 February 2017; Accepted: 28 February 2017; Published: 10 March 2017

Abstract: Two new two-dimensional (2D) layer coordination polymers—namely, $[Cd(L)_2]_n$ (**1**) and $[Co(L)_2(H_2O)]_n$ (**2**)—were synthesized by the reaction of corresponding metal salts with 3-(1*H*-imidazol-4-yl)benzoic acid (**HL**) incorporating 4-imidazolyl and carboxylate functional groups, and characterized by single-crystal X-ray diffraction, elemental analysis, IR spectroscopy, and powder X-ray diffraction (PXRD). Complex **1** is a 2D network with (4, 4) topology, while **2** is a typical 6^3-**hcb** topology net. Complex **1** exhibits intense light blue emission in the solid state at room temperature.

Keywords: 3-(1*H*-imidazol-4-yl)benzoate; 2D layer; coordination polymer; structural characterization

1. Introduction

In the last two decades, coordination polymers have become an expanding research topic in the fields of synthetic chemistry and materials science, not only because of their charming architectures and intricate topologies, but also their widely applications in numerous areas in fluorescence, magnetic properties, electrochemistry, gas adsorption/separation, catalysis, and so on [1–8]. The structure design methodology and properties of coordination polymers are mainly dependent on the intrinsic organic linkers [9,10], inorganic metal units, as well as the external synthesis conditions such as reaction temperatures, pH of the medium, reaction solvents, and counter anions [11–13]. Generally, organic linkers with N and/or O donors have often been utilized as effective building units in the process of coordination polymers [14,15]. In our previous studies, we make great efforts to design favourable organic ligands including imidazolyl- or carboxylate groups. For example, we designed the series of 4-imidazole-containing imidazole ligands and synthesized the porous coordination polymers based on the 4-imidazolate-metal building units, showing favourable gas selective adsorption property for CO_2 molecules [16,17]. Because of the diversity of the coordination modes of carboxylate groups, we deliberately design the difunction ligand 4-(1*H*-imidazol-4-yl)benzoic acid incorporating 4-imidazolyl and carboxylate functional groups that exhibit the diverse coordination modes because of these difunctional groups [18]. Two series of Cu(II) and Cd(II) coordination polymers are constructed based on 4-(1*H*-imidazol-4-yl)benzoic acid. As an extension of our previous work, we synthesized a new organic ligand-3-(1*H*-imidazol-4-yl)benzoic acid. Here, we report the synthesis and crystal structure of two new coordination polymers of $[Cd(L)_2]_n$ (**1**) and $[Co(L)_2(H_2O)]_n$ (**2**) obtained by the reaction of 3-(1*H*-imidazol-4-yl)benzoic acid (**HL**) with corresponding metal salts under hydrothermal condition.

2. Results and Discussion

*2.1. Structural Description of $[Cd(L)_2]_n$ (**1**)*

The X-ray single-crystal structural analysis reveals that $[Cd(L)_2]\cdot H_2O$ crystallizes in orthorhombic Pbcn space group. The asymmetric unit of **1** contains one crystallographically-independent Cd(II) atom, two L^- ligands, and one free lattice water molecule. As shown in Figure 1, the Cd1 centre with O4N2 binding set is coordinated by two pairs of oxygen atoms (O(1A), O(1B) and O(2A), O(2B)) of two chelating carboxylate groups from two distinct L^- ligands and two nitrogen atoms (N1, N1C) from other two L^- ligands, displaying a highly distorted octahedral coordination sphere. The Cd–O distances are 2.277(2) and 2.488(3) Å, while the Cd–N one is 2.265(3) Å, and the coordination angles around Cd(1) are in the range of 54.86(8)–144.02(8)° (Table 1). In this complex, each L^- ligand acts as a μ_2-bridge to link two Cd(II) atoms while each Cd(II) atom connects four different L^- ligands. In **1**, two L^- ligands and two Cd(II) ions form a macrocycle through the coordination bonds, where the lateral Cd···Cd distances are 8.33 Å, and the diagonal Cd···Cd distances are 10.01 and 13.33 Å, respectively. Thus, the shape of this macrocycle is a rhombus. In **1**, each L^- links two Cd(II) ions to form a two-dimensional (2D) (4, 4) net along the *ab* plane (Figures 2 and 3). And the C–H···O (C(5)···O(2) 2.773(4) Å, C(5)–H(5)···O(2) 100°) hydrogen bond exist among the 2D layers highlighted in red dotted lines; particularly, the non-classic weak interaction (C(9)–H(9)···π, 2.756 Å) also exists between the two neighbouring 2D layers, which further links the 2D layers into a three-dimensional (3D) supramolecular polymer (Figure 4).

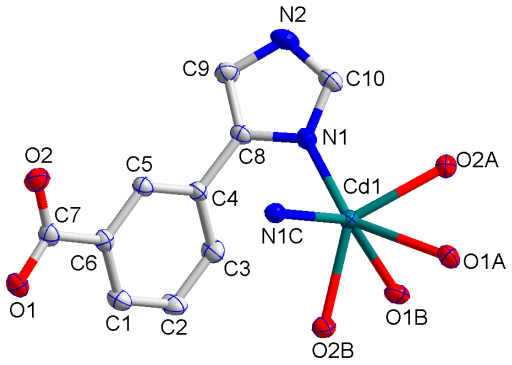

Figure 1. The coordination environment of Cd(II) ion in **1** with the ellipsoids drawn at the 30% probability level. The hydrogen atoms and free lattice water molecule are omitted for clarity. Symmetry code: A 0.5 + x, 0.5 + y, 0.5 − z, B 1.5 − x, 0.5 + y, z, C 2 − x, y, 0.5 − z.

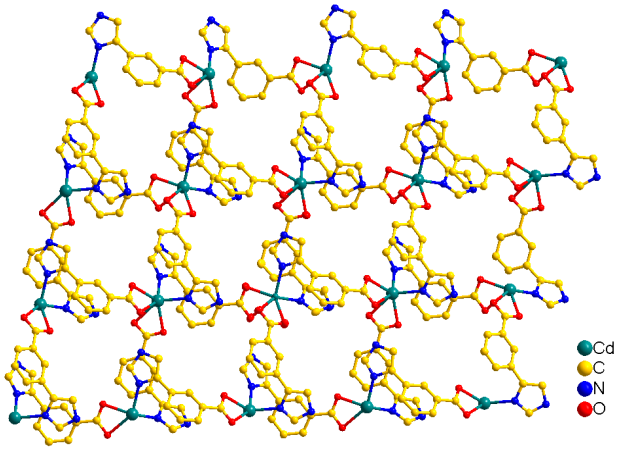

Figure 2. 2D layered structure of **1**.

Table 1. Selected bond lengths (Å) and bond angles (°) for **1** and **2**.

Bond	*d*	Bond	*d*
	1		
Cd(1)–N(1)	2.265(3)	Cd(1)–O(2) ii	2.277(2)
Cd(1)–O(1) i	2.488(3)		
	2		
Co(1)–O(1) i	2.0178(12)	Co(1)–N(3) ii	2.0667(14)
Co(1)–N(1)	2.1095(15)	Co(1)–O(4)	2.1667(12)
Co(1)–O(4)	2.1667(12)	Co(1)–O(5)	2.2327(13)
Angle	ω	**Angle**	ω
	1		
N(1) iii–Cd(1)–N(1)	96.46(13)	N(1) iii–Cd(1)–O(2) iv	124.03(10)
N(1)–Cd(1)–O(2) iv	89.19(9)	O(2) iv–Cd(1)–O(2) v	131.67(13)
N(1) iii–Cd(1)–O(1) v	144.02(8)	N(1)–Cd(1)–O(1)#3	102.62(10)
O(2) iv–Cd(1)–O(1) v	86.79(9)	O(2) v–Cd(1)–O(1) v	54.86(8)
O(1) v–Cd(1)–O(1) iv	79.06(15)		
	2		
O(1) iii–Co(1)–N(3) iv	99.42(6)	O(1) iii–Co(1)–N(1)	97.01(5)
N(3) iv–Co(1)–N(1)	92.00(6)	O(1) iii–Co(1)–O(4)	152.05(5)
N(3) iv–Co(1)–O(4)	107.27(5)	N(1)–Co(1)–O(4)	90.31(5)
O(1) iii–Co(1)–O(3)	92.96(5)	N(3) iv–Co(1)–O(3)	167.60(5)
N(1)–Co(1)–O(3)	87.26(5)	O(4)–Co(1)–O(3)	60.37(4)
O(1) iii–Co(1)–O(5)	87.23(5)	N(3) iv–Co(1)–O(5)	90.26(5)
N(1)–Co(1)–O(5)	174.81(5)	O(4)–Co(1)–O(5)	84.55(5)
O(3)–Co(1)–O(5)	89.53(5)		

Symmetry codes: (i) $-x+2, y, -z+1/2$; (ii) $x+1/2, y+1/2, -z+1/2$; (iii) $-x+1, -y+2, -z+1$; (iv) $-x+2, y+1/2, -z+3/2$; (iv) $-x+2, y-1/2, -z+3/2$.

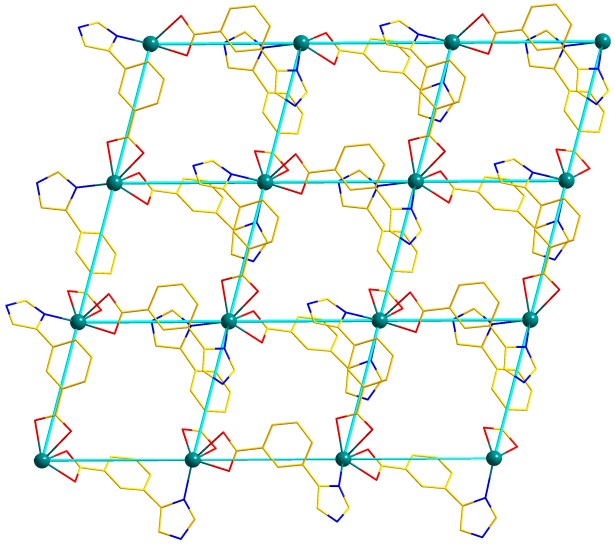

Figure 3. The 2D (4, 4) **sql** layered network of **1**.

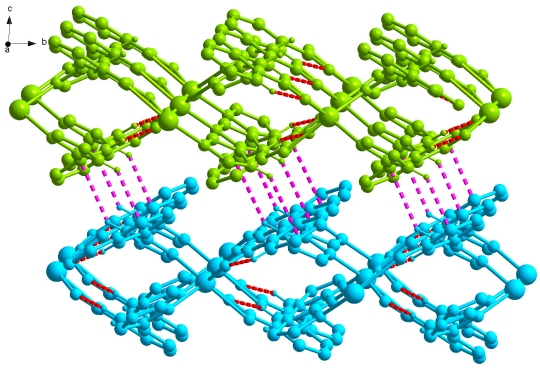

Figure 4. 3D supramolecular network structure of **1** linked by C-H···π stacking interactions.

*2.2. Structural Description of $[Co(L)_2(H_2O)]_n$ (**2**)*

When $Co(NO_3)_2{\cdot}6H_2O$, instead of $Cd(NO_3)_2{\cdot}4H_2O$ was used in the reaction, **2** with a different structure was isolated. Compound **2** crystallizes in the monoclinic space group $P2_1/c$. The asymmetric unit of **2** contains one crystallographically-independent Co(II) atom, two L^- ligands, and one coordinated water molecule. As shown in Figure 5, the Co1 has a distorted octahedral environment in which the equatorial plane contains O3, O4 atoms of one chelating carboxylate groups from one L^- ligand, and N3B, O1A from other two distinct L^- ligands, and the atoms N1 and O5 from L^- ligand and water molecules occupy the axial positions with an N1–Co1–O5 angle of 174.8° (Table 1). The two different L^- ligand employ as μ_2-bridge to link two Co(II) atoms, but two carboxylate groups adopting μ_1-η^1:η°-monodentate and μ_1-η^1:η^1-chelating coordination mode, respectively. In return, each Co(II) atom connected other three Co(II) atoms by the L^- ligand. Topologically, L^- ligands bridge the Co(II) atoms to form a 2D layer with 6^3-**hcb** topology where the Co(II) atom and L^- ligand act as 3- and 2-connected nodes, respectively (Figures 6 and 7). It is noteworthy that the NH or N atom of imidazolyl groups and the carboxylate group from L^- can be effective hydrogen bonding donors or acceptors in the construction of supramolecular structures. It can be clearly seen that the adjacent 2D layers are further linked by rich N–H···O, C–H···O hydrogen bonds (N(4)···O(2) 2.824(19) Å, N(4)–H(4)···O(2) 143°; O(5)···O(4) 2.787(18) Å, O(5)–H(5A)···O(4) 172°) to produce a 3D supramolecular polymer (Figure 8). Particularly, two benzene rings of the L^- ligands between the adjacent 2D layers are nearly parallel with a dihedral angle of 3.27° and are separated by a centroid–centroid distance of 3.58 Å, indicating the presence of π-π stacking interactions (Figure 8) [19].

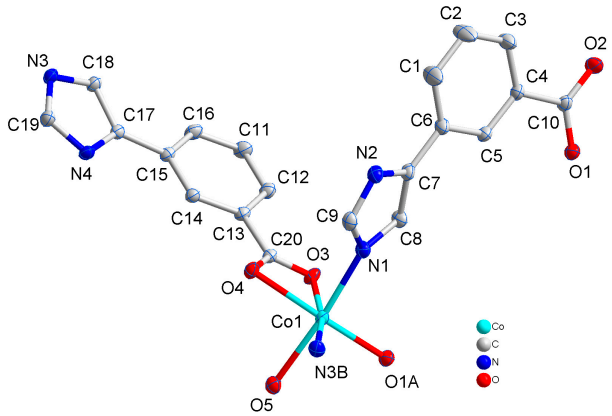

Figure 5. The coordination environment of Co(II) ion in **2** with the ellipsoids drawn at the 30% probability level. The hydrogen atoms are omitted for clarity. Symmetry code: A 1 − x, 2 − y, 1 − z, B 2 − x, 0.5 + y, 1.5 − z.

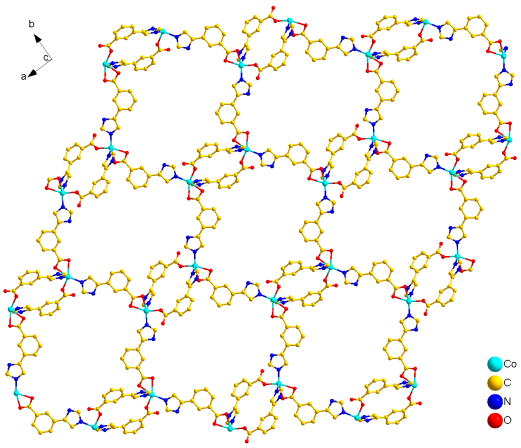

Figure 6. The 2D network structure of **2**.

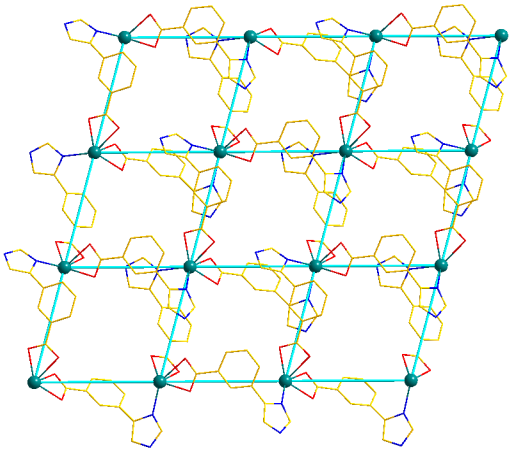

Figure 7. The representation of 6^3-**hcb** framework of **2**.

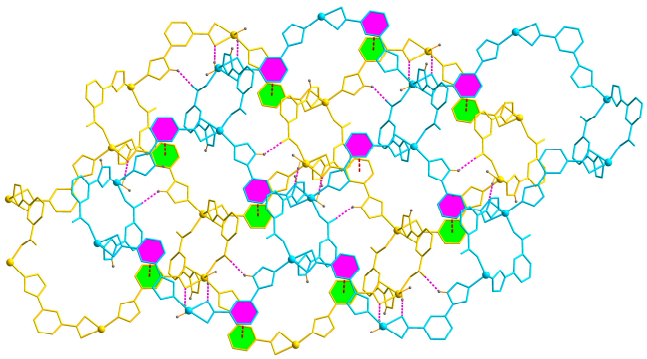

Figure 8. 3D supramolecular network structure of **2** linked by hydrogen bonds indicated by a dashed line and π-π stacking interactions of benzene groups.

2.3. Thermal Analysis and Powder X-ray Diffraction Analysis

Complexes **1** and **2** were subjected to thermogravimetric analysis (TGA) to ascertain the stability of supramolecular architecture, and the result is shown in Figure 9. No obvious weight loss was found for **1** before the decomposition of the framework occurred at about 405 °C, which is in good agreement with the results of the crystal structure. The first weight loss of 3.92% around 200 °C indicates the exclusion of coordinated water molecules (calc. 3.98%), and the decomposition of the residue occurred

at 370 °C for **2**. A powder XRD experiment was carried out to confirm the phase purity of bulk sample, and the experimental pattern of the as-synthesized sample can be considered comparable to the corresponding simulated one, indicating the phase purity of the sample (Figure 10). Furthermore, the thermal stability of **1** and **2** and the PXRD patterns under different temperatures were examined (Figure 10). The results imply that complexes **1** and **2** are stable up to 280 °C and 240 °C, respectively.

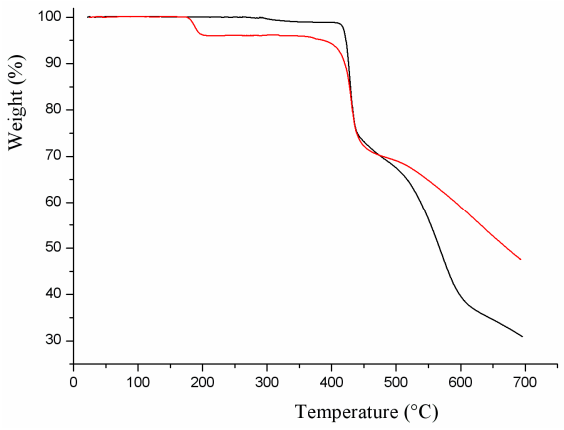

Figure 9. Thermal analysis curve of the complexes **1** and **2**.

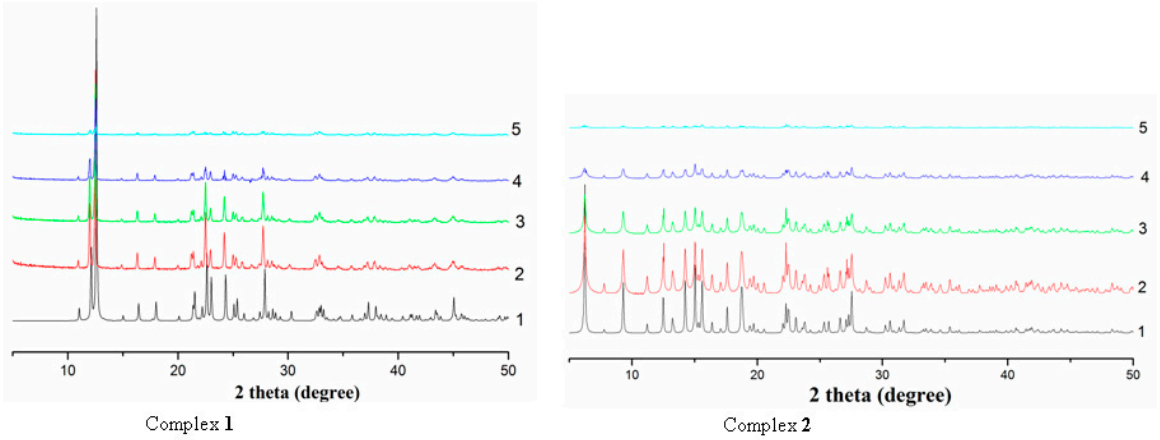

Figure 10. Powder X-ray diffraction patterns of complexes **1** and **2** at varied temperature. Complex **1**: 1. Simulated; 2. As-synthesized; 3. Experimental at 200 °C; 4. Experimental at 260 °C; 5. Experimental at 280 °C; Complex **2**: 1. Simulated; 2. As-synthesized; 3. Experimental at 150 °C; 4. Experimental at 210 °C; 5. Experimental at 240 °C.

2.4. Photoluminescent Property

Inorganic–organic hybrid complexes—especially comprising the d^{10} closed-shell metal centre and aromatic-containing system—have been intensively investigated for attractive fluorescence properties and potential applications, such as chemical sensors and photochemistry [20–23]. In this paper, the solid-state photoluminescent property of complex **1** has been investigated in the solid state at room temperature. Complex **1** exhibits light blue emission with maximum at 419 nm upon excitation at 320 nm as depicted in Figure 11, indicating that it may be a potential hybrid inorganic–organic photoactive material.

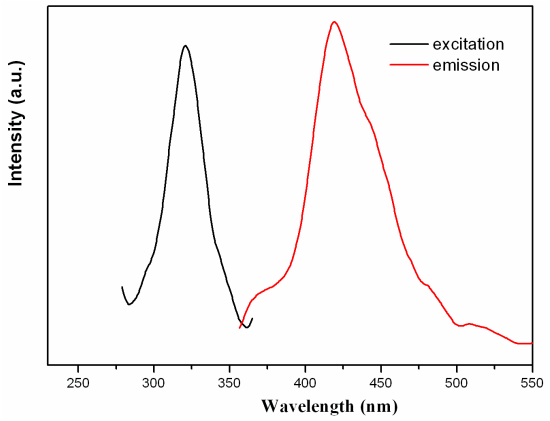

Figure 11. Solid-state photoluminescent spectra of **1** at room temperature.

3. Experimental Section

3.1. Materials and Instrumentation

All the commercially available chemicals and solvents were of reagent grade and used as received without further purification. Elemental analyses were performed on a Perkin-Elmer 240C Elemental Analyzer. IR spectra were recorded on a Bruker Vector 22 Fourier transform infrared (FT-IR) spectrophotometer (Bruker Instrument Inc., Karlsruhe, Germany) using KBr pellets. Thermogravimetric analyses (TGA) were performed on a simultaneous SDT 2960 thermal analyser (Thermal Analysis Instrument Inc., New Castle, DE, USA) under nitrogen with a heating rate of 10 °C·min^{-1}. Power X-ray diffraction (PXRD) patterns were measured on a Shimadzu XRD-6000 X-ray diffractometer (Shimadzu Corporation, Kyoto, Japan) with Cu$K\alpha$ (λ = 1.5418 Å) radiation at room temperature. The fluorescent spectra were measured using a Perkin Elmer LS-55B fluorescence spectrometer (PerkinElmer, Billerica, MA, USA).

*3.2. Synthesis of $[Cd(L)_2]_n$ (**1**)*

A mixture of HL (0.021 g, 0.1 mmol), $Cd(NO_3)_2{\cdot}4H_2O$ (0.0308 g, 0.1 mmol), and NaOH (0.004 g, 0.1 mmol) in 10 mL H_2O was sealed in a 20 mL Teflon-lined stainless steel container and heated at 120 °C for 72 h. Colourless block crystals of **1** were collected with a yield of 52% by filtration and washed with water and ethanol several times. Anal. Calcd. (%) for $C_{20}H_{14}N_4O_4Cd$: C, 49.35; H, 2.90; N, 11.51. Found (%): C, 49.53; H, 2.76; N, 11.39. IR(KBr): 3680–2750 (m), 1615 (s), 1535 (s), 1399 (s), 1188 (w), 1128 (m), 1094 (s), 950 (m), 853 (m), 785 (m), 701 (w), 650 (m), 506 (m) cm^{-1}.

*3.3. Synthesis of $[Co(L)_2(H_2O)]_n$ (**2**)*

Complex **2** was obtained by the same procedure used for the preparation of **1** except that the $Cd(NO_3)_2{\cdot}4H_2O$ was replaced by $Co(NO_3)_2{\cdot}6H_2O$ (0.029 g, 0.1 mmol). Purple block crystals of **2** were collected in 83% yield. Anal. Calcd. (%) for $C_{20}H_{16}N_4O_5Co$: C, 53.23; H, 3.57; N, 12.41. Found (%): C, 53.01; H, 3.62; N, 12.16. IR(KBr): 3650–2350 (m), 1598 (s), 1549 (s), 1371 (s), 1303 (w), 1225 (m), 1173 (m), 1072 (m), 975 (m), 837 (m), 781 (s), 712 (m), 627 (m), 587 (m), 518 (w) cm^{-1}.

3.4. Crystal Structure Determination

The single crystal data of $[Cd(L)_2]_n$ (**1**) and $[Co(L)_2(H_2O)]_n$ (**2**) were collected on a Bruker Smart APEX CCD diffractometer (Bruker, Billerica, MA, USA) with graphite-monochromated MoKα radiation (λ = 0.71073 Å) at 293(2) K. The structure was solved by direct method and refined by full-matrix least squares on F^2 using the SHELX-97 program [24]. The crystallographic data and structural refinement are listed in Table 2.

Table 2. Crystallographic data and structure refinement for **1** and **2**.

Empirical Formula	$C_{20}H_{14}N_4O_4Cd$	$C_{20}H_{16}N_4O_5Co$
Formula weight	486.75	451.30
Temperature/K	296(2)	296(2) K
Crystal system	Orthorhombic	Monoclinic
Space group	*Pbcn*	$P2_1/c$
a/Å	10.008(6)	14.201(2)
b/Å	13.330(8) A	19.000(3)
c/Å	14.580(9)	7.1599(11)
α/°	90	90
β/°	90	94.201(3)
γ/°	90	90
Volume/Å^3	1945(2)	1926.7(5)
Z	4	4
ρ_{calc} mg/mm^3	1.662	1.556
μ/mm^{-1}	1.157	0.932
S	1.026	1.029
$F(000)$	968	924
Index ranges	$-13 \leq h \leq 13$, $-17 \leq k \leq 17$, $-18 \leq l \leq 18$	$-18 \leq h \leq 10$, $-24 \leq k \leq 24$, $-9 \leq l \leq 9$
Reflections collected	19,008	13,088
Independent reflections	2244	4440
Data/restraints/parameters	2244/0/132	4440/0/276
Goodness-of-fit on F^2	1.026	1.029
Final R indexes ($I \geq 2\sigma$ (I))	$R_1 = 0.0397$, $wR_2 = 0.1217$	$R_1 = 0.0300$, $wR_2 = 0.0723$
Final R indexes (all data)	$R_1 = 0.0440$, $wR_2 = 0.1309$	$R_1 = 0.0365$, $wR_2 = 0.0757$
Largest diff. peak/hole/e·Å^{-3}	1.301/−0.731	0.404/−0.242

4. Conclusions

In summary, we successfully obtained two new coordination polymers $[Cd(L)_2]_n$ (**1**) and $[Co(L)_2(H_2O)]_n$ (**2**) by the reaction of corresponding metal salts with 3-(1*H*-imidazol-4-yl)benzoic acid incorporating 4-imidazolyl and carboxylate functional groups. Both complexes show 2D layer structures, and **1** is a (4, 4) topology net while **2** is a typical 6^3-**hcb** topology network. Furthermore, complex **1** exhibits blue photoluminescence emission at 419 nm upon excitation at 320 nm.

Supplementary Materials: Crystallographic data for the structure reported in this paper has been deposited with the Cambridge Crystallographic Data Centre as supplementary publication Nos. CCDC 1531060 for **1** and 1531061 for **2**. Copy of the data can be obtained free of charge on application to CCDC, 12 Union Road, Cambridge CB2 1EZ, UK (Fax: +44-1223-336-033; E-Mail: deposit@ccdc.cam.ac.uk).

Acknowledgments: This project was supported by Natural Science Foundation of Fuyang (KJ2011B123).

Author Contributions: Xing-Zhe Guo, Zi-Long Li and Shan-Shan Shi synthesized the metal coordination polymers. Zi-You Zhang analysed the crystal data of coordination polymers. Shui-Sheng Chen designed the method and guided the manuscript.

Conflicts of Interest: The authors declare no conflict of interest.

References

1. Kitagawa, S.; Matsuda, R. Chemistry of coordination space of porous coordination polymers. *Coord. Chem. Rev.* **2007**, *251*, 2490–2509. [CrossRef]
2. Férey, G. Hybrid porous solids: Past, present, future. *Chem. Soc. Rev.* **2008**, *37*, 191–214. [CrossRef] [PubMed]
3. Long, J.R.; Yaghi, O.M. The pervasive chemistry of metal–organic frameworks. *Chem. Soc. Rev.* **2009**, *38*, 1213–1214. [CrossRef] [PubMed]

4. Chen, S.S.; Wang, P.; Takamizawa, S.; Okamura, T.A.; Chen, M.; Sun, W.Y. Zinc(II) and cadmium(II) metal-organic frameworks with 4-imidazole containing tripodal ligand: Sorption and anion exchange properties. *Dalton Trans.* **2014**, *43*, 6012–6020. [CrossRef] [PubMed]
5. Farha, O.K.; Hupp, J.T. Rational design, synthesis, purification, and activation of metal–organic framework materials. *Acc. Chem. Res.* **2010**, *43*, 1166–1175. [CrossRef] [PubMed]
6. Chen, S.S.; Sheng, L.Q.; Zhao, Y.; Liu, Z.D.; Qiao, R.; Yang, S. Syntheses, structures, and properties of a series of polyazaheteroaromatic core-based Zn(II) coordination polymers together with carboxylate auxiliary ligands. *Cryst. Growth Des.* **2016**, *16*, 229–241. [CrossRef]
7. Furukawa, H.; Cordova, K.E.; O'Keeffe, M.; Yaghi, O.M. The chemistry and applications of metal-organic frameworks. *Science* **2013**, *341*, 974. [CrossRef] [PubMed]
8. Grancha, T.; Ferrando-Soria, J.; Castellano, M.; Julve, M.; Pasán, J.; Armentano, D.; Pardo, E. Oxamato-based coordination polymers: Recent advances in multifunctional magnetic materials. *Chem. Commun.* **2014**, *50*, 7569–7585. [CrossRef] [PubMed]
9. Chen, S.S. The roles of imidazole ligands in coordination supramolecular systems. *CrystEngComm* **2016**, *18*, 6543–6565. [CrossRef]
10. Zeng, W.; Jiang, J. Synthesis and crystal structures of two novel O, N-containing spiro compounds. *Crystals* **2016**, *6*, 69–75. [CrossRef]
11. Qiao, R.; Chen, S.S.; Sheng, L.Q.; Yang, S.; Li, W.D. Syntheses, crystal structures, and properties of four complexes based on polycarboxylate and imidazole ligands. *J. Solid State Chem.* **2015**, *228*, 199–207. [CrossRef]
12. Suckert, S.; Germann, L.S.; Dinnebier, R.E.; Werner, J.; Näther, C. Synthesis, structures and properties of cobalt thiocyanate coordination compounds with 4-(hydroxymethyl)pyridine as Co-ligand. *Crystals* **2016**, *6*, 38–54. [CrossRef]
13. Kamari, A.A.; Haque, R.A.; Razali, M.R. A heterobimetallic 2-D coordination polymer $[Na_2(Cu_2I_2(2pyCOO)_4)(H_2O)_4]_n$ (2pyCOO$^-$=picolinate) within a 3-D supramolecular architecture. *Crystals* **2016**, *6*, 96–102. [CrossRef]
14. Wang, X.P.; Han, L.L.; Lin, S.J.; Li, X.Y.; Mei, K.; Sun, D. Synthesis, structure and photoluminescence of three 2D Cd(II) coordination polymers based on varied dicarboxylate ligand. *J. Coord. Chem.* **2016**, *69*, 286–294. [CrossRef]
15. Tai, X.S.; Wang, X. Synthesis and crystal structure of a 1D chained coordination polymers constructed from Ca^{2+} and 2-[(E)-(2-furoylhydrazono)methyl]benzenesulfonate. *Crystals* **2015**, *5*, 458–465. [CrossRef]
16. Chen, S.S.; Chen, M.; Takamizawa, S.; Chen, M.S.; Su, Z.; Sun, W.Y. Temperature dependent selective gas sorption of the microporous metal-imidazolate framework [Cu(L)] [H_2L = 1,4-di(1H-imidazol-4-yl) benzene]. *Chem. Commun.* **2011**, *47*, 752–754. [CrossRef] [PubMed]
17. Chen, S.S.; Chen, M.; Takamizawa, S.; Wang, P.; Lv, G.C.; Sun, W.Y. Porous cobalt(II)-imidazolate supramolecular isomeric frameworks with selective gas sorption property. *Chem. Commun.* **2011**, *47*, 4902–4904. [CrossRef] [PubMed]
18. Chen, S.S.; Liu, Q.; Zhao, Y.; Qiao, R.; Sheng, L.Q.; Liu, Z.D.; Yang, S.; Song, C.F. New metal-organic frameworks constructed from the 4-imidazole-carboxylate ligand: Structural diversities, luminescence, and gas adsorption properties. *Cryst. Growth Des.* **2014**, *14*, 3727–3741. [CrossRef]
19. Chen, S.S.; Qiao, R.; Sheng, L.Q.; Zhao, Y.; Yang, S.; Chen, M.M.; Liu, Z.D.; Wang, D.H. Cadmium(II) and zinc(II) complexes with rigid 1-(1H-imidazol-4-yl)-3-(4H-tetrazol-5-yl)benzene and varied carboxylate ligands. *CrystEngComm* **2013**, *15*, 5713–5725. [CrossRef]
20. Wang, D.Z.; Fan, J.Z.; Jia, D.; Du, C.C. Zinc and cadmium complexes based on *bis*-(1Htetrazol-5-ylmethyl/ylethyl)-amine ligands: Structures and photoluminescence properties. *CrystEngComm* **2016**, *18*, 6708–6723. [CrossRef]
21. Takashima, Y.; Martínez, V.M.; Furukawa, S.; Kondo, M.; Shimomura, S.; Uehara, H.; Nakahama, M.; Sugimoto, K.; Kitagawa, S. Molecular decoding using luminescence from an entangled porous framework. *Nat. Commun.* **2011**, *2*, 168–172. [CrossRef] [PubMed]
22. Ferrando-Soria, J.; Khajavi, H.; Serra-Crespo, P.; Gascon, J.; Kapteijn, F.; Julve, M.; Lloret, F.; Ruiz-Pérez, C.; Journaux, Y.; Pardo, E. Highly selective chemical sensing in a luminescent nanoporous magnet. *Adv. Mater.* **2012**, *24*, 5625–5629. [CrossRef] [PubMed]

23. Hu, Z.; Deiberta, B.J.; Li, J. Luminescent metal–organic frameworks for chemical sensing and explosive detection. *Chem. Soc. Rev.* **2014**, *43*, 5815–5840. [CrossRef] [PubMed]
24. Sheldrick, G.M. A short history of SHELX. *Acta Cryst.* **2008**, *A64*, 112–122. [CrossRef] [PubMed]